Geomechanics and Engineering, *Vol. 41, No. 2 (2025) 319-325*
https://doi.org/10.12989/gae.2025.41.2.319

Analysis on lateral resistance of precast bored piles based on experimental and numerical approach

Dohyun Kim*

Department of Civil and Environmental Engineering, Hanbat National University, Daejeon 34158, Korea

(*Received December 7, 2024, Revised April 7, 2025, Accepted April 9, 2025*)

Abstract. Full scale field tests were performed on test piles installed based on a typical installation procedure of a precast bored piles, with various cement layer thickness and water-cement ratio of the cement slurry along the pile shaft. The results of the field test were compared to the test conducted on test pile following the installation procedure of driven piles. Simultaneously, large deformation finite element analysis was carried out to verify the effectiveness of precast bored piles under lateral loadings. Lateral displacement of the pile head was reduced as the thickness of the cement layer along the pile shaft increases, up to a certain thickness. Also, lower water-cement ratio also decreased the pile head displacement, but was found to have less effect compared to the cement layer thickness. Overall, the results show that the application of precast bored piles was found to be more effective in reducing the lateral displacement of the pile head under higher lateral loading.

Keywords: full-scale test; large deformation analysis; lateral displacement; lateral load; precast bored piles

1. Introduction

Recently, the number of hazardous events occurred in Korea has risen significantly. In case of earthquakes, the case occurred during the 1978 – 1999 period was 19.1 cases per year. As for the number of cases occurred after the year 1999, it was approximately 71 cases per year, which was more than three times in comparison. Moreover, if the number of earthquakes is limited to the cases over 3.0 magnitude, average number of earthquakes in the past ten-year period has risen more than 300% (7/year→28.4/year) (Korea Meteorological Administration 2023). Also, the increase in precipitation during the past 1-year period due to climate change was measured to be 8.5%, which was the cause for landslides, debris flow, embankment failures and other incidents lowering the integrity of the whole social infrastructure system. However, based on the projection under the assumption that the energy and natural resource consumption rate is kept constant, increase in extreme rainfall events will rise 30% by 2040 and 53% by 2100 compared to 2021 (Han *et al*. 2018, Korea Presidential Water Commission 2024).

Hazardous and extreme events mentioned above have a critical effect on the performance and the structural stability of infrastructures as they act as a lateral load, causing bending and tensile failures. For this reason, it is crucial that the pile foundation design should focus on the displacement and resistance under lateral loading condition, as well as axial capacity. Moreover, conventional pile installation based on driving is not specifically suitable to deal with excessive lateral loading, as well as cause severe damage to the structural integrity and the serviceability to a pile.

To overcome the mentioned limitations and threats, the use of precast bored pile (PBP) can be the solution. PBP uses manufactured (precast) piles in which the quality control can be easily achieved. Since PBPs are installed by placing the precast piles in the borehole rather than driven in, the possibility of damaging the pile can be significantly reduced, which is reported to be a problem in structural stability. This can also reduce the noise and vibration during installation. For this reason, the substitution of conventional driven piles to PBP has become common in major urban centers in Korea, Japan, and Singapore (Kumara *et al.* 2016, Lee *et al*. 2016, Jung *et al.* 2017, Kim *et al.* 2018, Kim *et al.* 2020, Jeong *et al*. 2021). Moreover, the lateral resistance of the PBP can be secured even under extreme conditions due to the distinct installation procedure of injecting cement paste along the shaft of the pile. Kim *et al.* (2020) examined and studied the increase in lateral resistance of PBP through field tests and numerical analysis.

In this study, the lateral resistance of steel pipe PBP will be rigorously investigated through full-scale tests to observe its effectiveness under lateral loading. The effectiveness of lateral resistance of the PBP with additional cement layer along the shaft will be quantified by normalizing the test results with the test results done on test pile set identical to the driven pile conditions (no cement layer along the shaft). Simultaneously, large deformation finite element analysis will also be carried out for parametric studies, as well as verify the test results.

2. Precast bored piles

The precast bored pile has a unique installation process of injecting an additional cement layer along the shaft of the pile (Fig. 1). However, compared to driven piles and drilled

*Corresponding author, Assistant Professor
E-mail: geokim@hanbat.ac.kr

ISSN: 2005-307X (Print), 2092-6219 (Online)

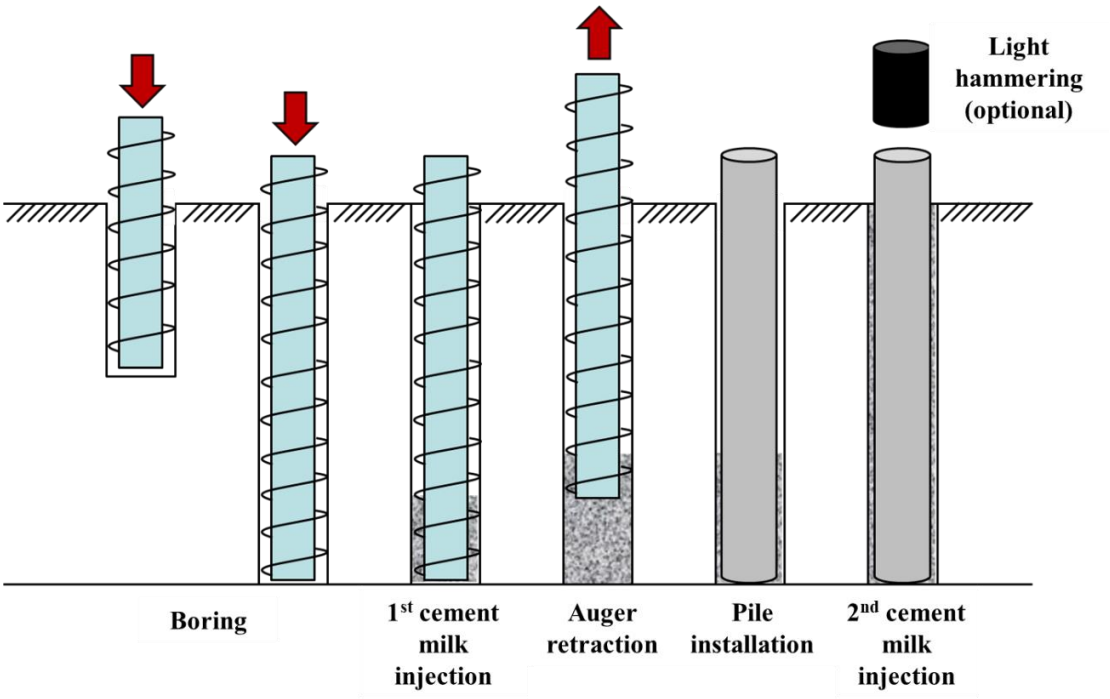

Fig. 1 Precast bored pile installation procedure

Table 1 Mechanical properties at test site

Soil type		Unit weight (kN/m^3)	Elastic modulus (MPa)	Poisson's ratio	Cohesion (kPa)	Internal friction angle (°)
Fill		17	10	0.35	0	25
Sedimentary layer		18	10	0.32	15	27
Weathered soil		19	65	0.32	21	31
Weathered rock		21	250	0.30	30	33
Soft rock		24	1,000	0.25	150	35
Cement slurry	80%	20	2,700	0.20	-	-
	120%	19	2,000	0.25	-	-

shafts, studies on PBP, let alone real-scale pile loading test, have only been carried out recently on limited number of cases (Kim 2018, Kim *et al*. 2020). Studies on PBP have been limited on providing empirical formulas roughly predicting the bearing capacity based on the SPT-N value of the surrounding soil or rocks (Jeong *et al*. 2021).

Deformation based studies, such as analysis of the load-settlement and load-transfer (f-w) curves, have not been rigorously carried out. Deformation of bored piles including PBP has only been estimated based on theoretical approaches which implies uncertainties and assumptions, which is inevitable when applying approaches developed for different piling methods (Reese and O'Neill, 1988). For this reason, wider use and application of PBP is not being fulfilled despite the fact that PBP provides higher and more stable support.

Some recent studies focused on the additional cement layer and concluded that the PBP shows higher shaft resistance compared to driven piles through experiments and numerical analysis (Park *et al*. 2004, Kim 2018, Kim *et al*. 2020). It was also found that the PBP shows higher pullout resistance through experimental results (Park and Chun 2016). However, the even though some studies focused on the behavior of PBP under lateral loading (Hong *et al*. 1999), lateral resistance of the PBP considering various shaft conditions – cement layer thickness, water-cement ratio of cement layer – were not properly tested nor studied.

3. Full-scale field test

In order to investigate the effectiveness of the PBP's resistance under lateral loading, total of 4 cases (three test piles installed under PBP condition and one under driven pile condition) of full-scale field test were carried out.

3.1 Ground condition

The field test was conducted on a site with mostly sandy soils. Based on the ground investigation, it was found that the soil profile consists of fill (0 m ~ 1.5 m), sedimentary

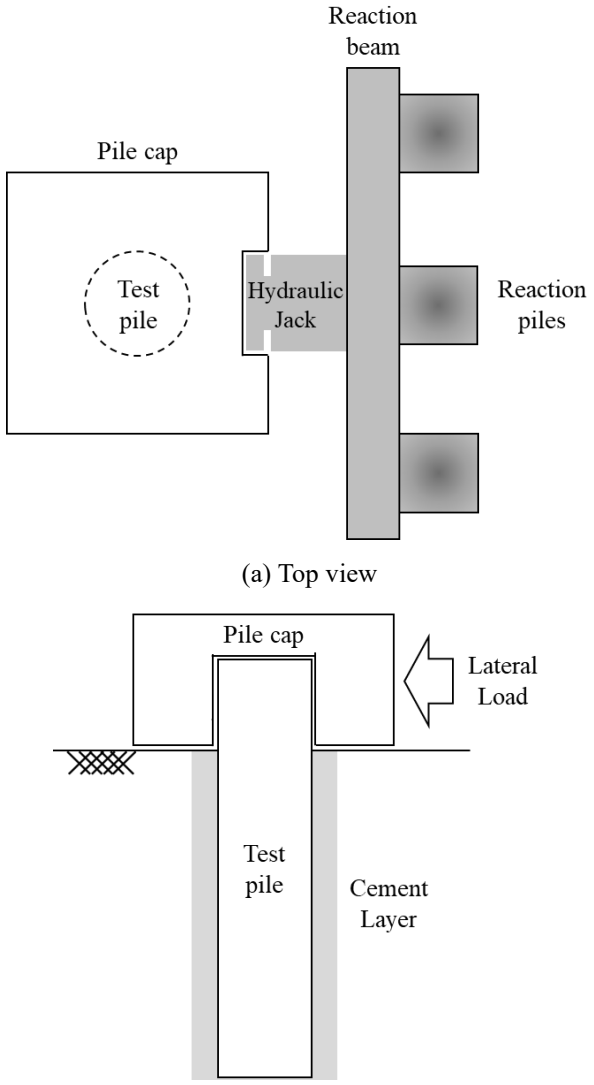

(a) Top view

(b) Side view

Fig. 2 Field test preparation

layer (1.5 m ~ 4 m), weathered soil (4 m ~ 12 m), weathered rock (12 m ~ 20 m) and soft rock layer (20 m ~). The lower 85% mechanical properties of the layers and the cement slurry are shown in Table 1 (Kim 2018, Kim *et al*. 2020).

3.2 Test preparation and procedure

The test pile was set to 20 m, and the pile tip was placed on the top of the soft rock layer. Fig. 2 shows the installation condition of the test pile and the lateral loading system. The field test was conducted by applying a lateral load at the pile cap which transfers the load to the head of the test pile. The lateral loading is applied to the test pile up to 6 tons over 12-minute period through a hydraulic jack which pushes against a reaction beam supported by three reaction piles. The hydraulic jack applies the lateral load on the pile cap through a slot which is optimally aligned with the center of the test pile, preventing any asymmetric loading. 10 strain gauges, protected by a metal casing, measuring the lateral displacement were installed along the two sides of the shaft, with 5 m spacing from the pile head to the pile tip below the ground level (0 m (pile head), -5 m, -10 m-15 m, -20 m).

Table 2 Test and numerical cases and conditions

	W/C (%)	Thickness (mm)
Test 1 / Numerical 1	80	200
Test 2 / Numerical 2	80	50
Test 3 / Numerical 3	120	200

3.3 Test cases and conditions

Table 2 states the two major parameters this study will focus on – the water-cement ratio of the cement and the thickness of the cement layer along the shaft of the test pile. For test case 1 and numerical case 1, the water-cement ratio of the injected cement will be set to 80%, which is close to the recommended water-cement ratio requirements of the precast bored piles of 83%. The thickness of the cement layer is set to 200 mm which is thicker than the recommended cement layer thickness for precast bored piles of 50 mm. Test and numerical case 2 has a test condition of water-cement ratio of 80% and the thickness of cement layer of 50 mm, which is the recommended thickness of PBP in actual engineering practice. Finally, for the third test and numerical case, the water-cement ratio of the injected cement was set to 120%, which is significantly blender than the recommended cement mixture (however, it is equivalent to uniaxial compression strength of 490 kPa, which is the minimum requirement according to PBP field manual) (Korea Land and Housing Corporation 2016). And the thickness of the cement layer was set to 200 mm. Through this, the effectiveness of using PBP under lateral loading and the effect of major influence factors will be quantified and studied.

3.4 Test results

The field test results will be stated based on a new concept called “Resistance ratio”. The resistance ratio will be defined as the following

$$2 - D_{PBP} / D_{DP} \quad (1)$$

where, D_{PBP} is the lateral displacement measured from a test PBP and D_{DP} is the lateral displacement is the measurement of a test pile representing a driven pile (no cement layer). This indicator will display the test results in the form of increased lateral resistance or decrease in lateral displacement by using PBPs compared to driven piles.

Table 3 shows the test results conducted in this study. Based on the test results it was clear that the cement layer along the shaft of the PBP has a notable effect in decreasing the displacement of the pile under lateral loading. Moreover, among the major influence factors the thickness of the cement layer was found to have greater effect on the lateral resistance of PBP compared to the water-cement ratio of the injected cement. By increasing the thickness of

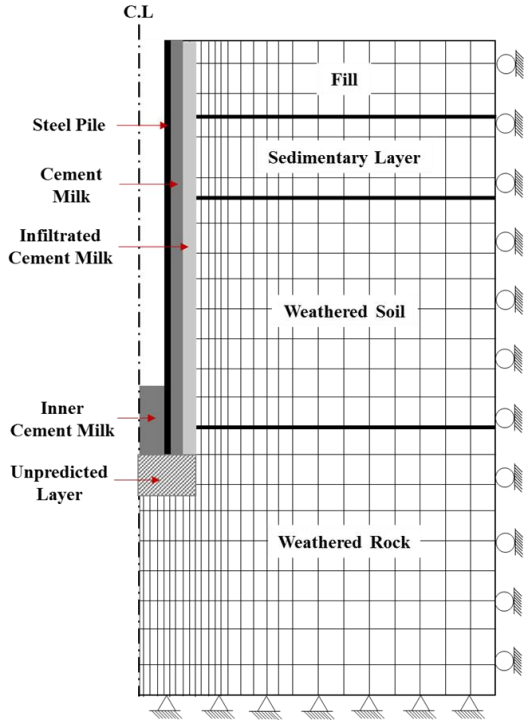

Fig. 3 Numerical modelling

the cement layer from 50 mm to 200 mm, the increase in resistance ratio was approximately 101%, doubling the lateral resistance by using PBPs. However, when the water-cement ratio of the cement changes from 80% to 120% (weaker cement layer) the resistance ratio decreases about 36%, showing more lateral displacement.

Finally, in all cases the lateral displacement (resistance ratio) of test piles was found to show similar number in all the PBP and driven pile test conditions below the depth of 15 m.

4. Numerical analysis

Along with the field test, 3D numerical analysis was also carried out to establish a numerical model simulating the lateral behavior of PBP.

4.1 FE mesh, elements and boundaries

In this study, adequate mesh design is critical, especially when it involves lateral movements and excessive deformation of meshes around the piles. To enhance the accuracy of the numerical analysis, various elements observed in the site investigation and field test are included in the analysis, such as cement layer. Due to symmetry, only a quarter of a whole mesh was used in the three-dimensional analyses to save calculation time and memory space. For the three-dimensional finite element analysis (FEA), the pile and the soil were modeled by 27-noded second-order brick elements, with the pile as linear elastic material and the soil based on Mohr-Coulomb model. Fig. 3 shows the schematic of the mesh in 2D form along with the boundary conditions. Note that the unpredicted layer at the

Table 3 Test results

Depth (m)	Resistance ratio		
	Test 1	Test 2	Test 3
0	1.4021	1.2001	1.2575
-5	1.1380	1.0687	1.0850
-10	1.0303	1.0102	1.0163
-15	1.0000	1.0000	1.0000
-20	1.0000	1.0000	1.0000

pile tip will be substituted with the soil condition at the corresponding depth. The overall dimension of the model boundaries comprises a width of 15 times the pile diameter (D) to eliminate the influence of boundary effect on the pile behavior (O'Neill *et al*. 1996). The dimension if the model mesh was designated based on the case study prior to the actual analysis.

4.2 Auto-remeshing method

Auto-remeshing numerical approach can avoid severe mesh distortion and calculation failure under large deformation analysis by updating the finite element mesh and the stress state before the unwanted mesh distortion and prevent computational failure. Although the auto-remeshing numerical method may not be fully capable of simulating the continuous loading process, it has been proved by numerous studies and research that it is capable of simulating and predicting the ground response on various geotechnical issues (Hu and Randolph 1998, Tian *et al.* 2014, Wang *et al.* 2015, Kim *et al*. 2023).

The automated remeshing process is independently implemented using a set of object-oriented language, PYTHON (Van Rossum and Drake 2006) script that can be used in ABAQUS scripting interface. The proposed procedure implemented in the scripts contain specification of multiple variables to a specific geometry, elements, boundary conditions, target displacements. The initial processes, which is model development and initial analysis, are mostly done manually, using the CAE option. After the initial analysis, the rest of the process is automated using the developed scripts. When the main script is called for the first time, it checks whether the targeted excavation length has been reached. If it is reached, a set of other scripts are applied to automatically iterate through all outputs of the first step. If the targeted excavation length is not reached, then a new step and mesh is created by invoking the following ABAQUS scripting interface command:

Mdb.Model(name=*newmodel*,objectToCopy=mdb.models[*oldmodel*])

where, *oldmodel* is the variable containing the name of the previous model, and *newmodel* is the variable containing the new model name in which the step number is incrementally updated (i + 1). This process is continued till the targeted lateral loading is completed. Fig. 4 shows the flow chart of the auto RITSS method applied in this study (Orazalin 2017, Orazalin and Whittle 2018, Kim 2024).

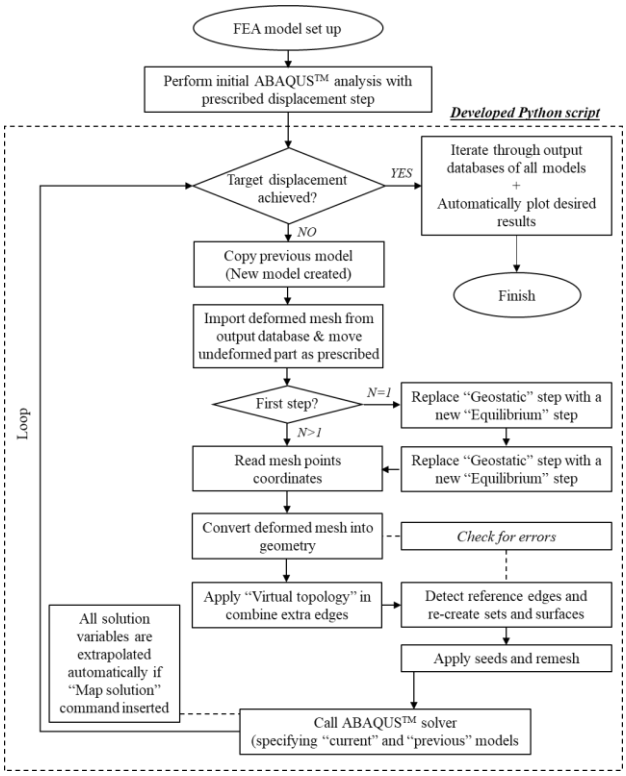

Fig. 4 Flow chart of the auto-remeshing process

4.3 Interface modelling

To fully consider the lateral behavior of the PBP and reflect the actual interfaces of the field test site, special effort was given to interface models between the steel test pile-cement slurry around and inside the pile-soil-cement layer-soil to simulate the specific characteristic of the PBP through t-z curves proposed for PBPs (Kim 2018, Kim *et al.* 2020). The proposed t-z curve that considers the relative settlement between each of the elements and cement slurry infiltration was designated by using the ABAQUS user-subroutine option "FRIC". Different relative settlement and the maximum shear stress and brittle behavior were modelled for each interface. Interfaces based on the proposed t-z curve were modelled between pile-cement layer, cement layer-soil-cement layer, and soil-cement layer-soil.

4.3.1 Pile – cement layer

Due to the cement slurry cast in the borehole, the shaft resistance of the PBP is much greater than the skin friction of a driven pile. Additionally, the shear stress acting between the pile and the cement slurry layer is relatively higher than the shear stress acting between the elements. This condition was confirmed through the tests carried out in previous studies (Kim 2018, Kim *et al*. 2020). To simulate the actual behavior of the interface between the pile and the cement slurry, we assumed a 'hard contact', which has infinite shear stress and failure does not occur.

4.3.2 Cement layer – soil-cement – soil

The interface between the cement layer and the soil was modelled based on the proposed t-z curve considering relative displacement and t-z curve which considers the excessively high shear strength and brittle behavior due to cement slurry infiltration. The interface between the cement slurry and soil is modelled in two different types.

Table 4 Relative settlement (Broms 1979)

Soil layer	Relative settlement (mm)
Fill	7
Sedimentary layer (SM)	4.5
Sedimentary layer (GP)	4
Weathered soil	3.5
Weathered rock	2
Soil-cement layer	1

The length of the relative settlement differs according to the types of soil in which the pile is socketed as shown in Table 4 (Broms 1979, Briaud *et al*. 1991). In case where a soil-cement layer is present, the relative displacement is significantly smaller, as in rocks. This assumption reflects the failure mechanism observed from the small-scale field test. Through the small-scale field test, we showed that the cement slurry infiltrated into the soil, and the failure surface occurred between the hardened cement slurry and soil. The maximum shear stress (τ_{max}) of the type 1 after the elastic slip section is estimated based on the earth pressure (p') and the friction coefficient (μ). Eq. (2) shows the estimation of τ_{max} and the friction coefficient (μ) is estimated based on following Eqs. (3) and (4).

$$\tau_{max} = \mu \times p \tag{2}$$

$$\mu = \tan\delta \tag{3}$$

$$\delta = tan^{-1}\left(\frac{sin\varphi \times cos\varphi}{1 + sin^2\varphi}\right) \tag{4}$$

where, δ is the interface friction angle and φ is the friction angle of the soil layer.

However, due to the hardening process of the cement slurry, additional adhesive strength was considered in the analysis between the cement layer and the soil-cement layer. Based on the field measurement and laboratory tests, the peak shear stress (τ_{peak}) of the brittle type proposed experimental load-transfer curve is in the range of 40~60% of the shear strength of cement slurry (Kim 2018, Kim *et al.* 2020).

In the early stage of the loading test, the shear strength between the cement and the soil increases based on the elastic behavior. Additionally, due to the light hammering done at the end of the pile installation, no significant settlement in the base of the pile was observed. To simulate the pile loading process, different interface behaviors were modelled based on the type of soil.

4.4 Analysis results

In carrying out the numerical analysis, the modelling was executed identical to the field test conditions. And the soil properties were based on Table 1.

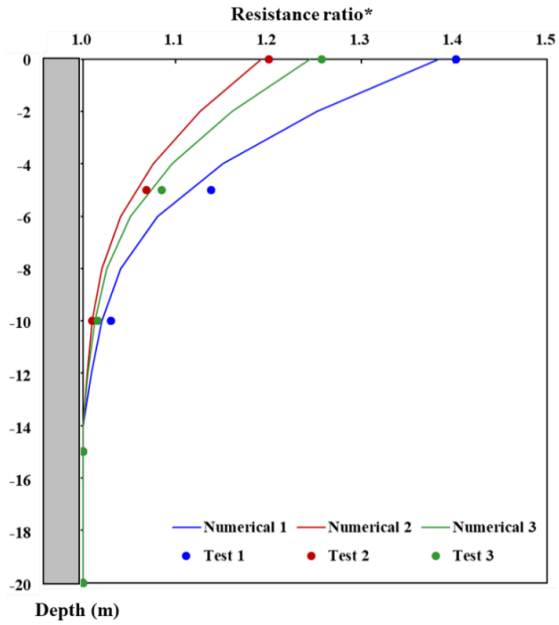

Fig. 5 Test and numerical results

Table 5 Numerical analysis results

Depth (m)	Resistance ratio		
	Test 1	Test 2	Test 3
0	1.3831	1.1921	1.2445
-2	1.2520	1.1260	1.1607
-4	1.1512	1.0756	1.0964
-6	1.0806	1.0403	1.0514
-8	1.0405	1.0203	1.0258
-10	1.0202	1.0101	1.0129
-12	1.0090	1.0050	1.0057
-14	1.0000	1.0000	1.0000
-16	1.0000	1.0000	1.0000
-18	1.0000	1.0000	1.0000
-20	1.0000	1.0000	1.0000

Identical to the field test results, the numerical analysis results are also presented as resistance ratio, which is derived by normalizing the lateral displacement of the PBP model with numerical results of a driven pile model.

The numerical results are shown in Fig. 5 in terms of load-displacement curves and on Table 5. Note that, in Fig. 6 while the y-axis shows the depth below the ground surface, the x-axis shows the resistance ratio, not the lateral displacement. So, when the results show higher value in the x-axis, it means that the resistance ratio is high, thus less lateral displacement. By comparing the test and numerical results it can be concluded that the numerical model used in this study is capable of simulating the behavior of PBP under lateral loading. Test results and the numerical calculation results show similar tendencies on lateral displacement. In all three cases the difference in lateral displacement is found to be bigger at the pile head (i.e., higher resistance ratio) and as it gets closer to the pile tip lateral displacement between PBP and driven pile measured to be similar (i.e., lower resistance ratio, closer to value of 1.0).

According to Fig. 5, it was found that the numerical calculation tends to underestimate the effectiveness of using PBP, showing slightly lower resistance ratio. This may be due to the fact that the applied soil properties are based on a lower 85% value obtained from the field investigation of the test site. However, since the numerical analysis results tend to underestimate the lateral resistance of PBP, it can be safe to say that the numerical model applied in this study can be used in planning, design and analyzing the lateral performance of PBP, as it provides conservative (safe-side) results.

5. Conclusions

This study investigates the increase in lateral resistance capacity of PBPs compared to driven piles through real-scale field tests and rigorous numerical analysis considering the large deformation behavior. All results were stated based on a concept called “resistance ratio”, a normalized lateral displacement of PBP-based test piles with driven pile-based test pile. Based on the 4 field test results and numerical computed results, the following conclusions can be drawn:

• Due to the unique installation procedure of the PBP, injection of cement paste along the shaft of the pile, additional cement layer is formed and this changes the lateral behavior of PBP.

• Based on the field test, it was found that the major influence factor is the thickness of the cement layer and the water-cement ratio of the injected cement.

• Among the major influence factors, the thickness of the cement layer was found to have greater effect on the lateral behavior of PBP.

• In all field test cases, the PBP was shown to have superior resistance against lateral loading compared to driven piles at pile head.

• Numerical model focusing on the interface modelling along the shaft of the PBP was found to simulate and predict the behavior of PBP under lateral loading, as well as under axial loading.

Acknowledgments

The research described in this paper was financially supported by the National Research Foundation of Korea (NRF) under the research project No.RS-2022-00166673, and the author expresses its gratitude.

References

ABAQUS CAE (2019), User’s manual, Dassault Systemes Simulia, Rhode Island, USA.

Briaud, J.L., Jeong, S. and Bush R. (1991), “Group effect in the case of downdrag”, Geotechnical Engineering Congress, Geotechnical Special Publication, **27**, 505-518.

Broms, B. (1979), "Negative skin friction", *Proceedings of the 6th Asian Regional Conference of Soil Mechanics and Foundation Engineering*, Singapore.

Han, J., Shim, C. and Kim, J. (2018), "Variance analysis of RCP4.5 and 8.5 ensemble climate scenarios for surface temperature in South Korea", *J. Climate Change Res*., **9**(1), 103-115. https://doi.org/10.15531/KSCCR.2018.9.1.103.

Hu, Y. and Randolph, M.F. (1998), "A practical numerical approach for large deformation problems in soil", *Int. J. Numer. Anal. Method. Geomech*., **22**(5), 327-350.

Jeong, S., Kim, D. and Park, J. (2021), "Empirical bearing capacity formula for steel pipe prebored and precast piles based on field tests", *ASCE Int. J. Geomech*., **21**(9). https://doi.org/10.1061/(ASCE)GM.1943-5622.0002112.

Jung, G., Kim, D., Lee, C. and Jeong, S. (2017), "Analysis of skin friction behavior in prebored and precast piles based on field loading test", *J. Korean Geotech. Soc*., **33**, 31-38.

Kim, D. (2018), "Proposed shaft resistance of prebored and precast pile using field loading test", Ph.D thesis, Yonsei University, Seoul, Republic of Korea.

Kim, D. (2021), "Large deformation finite element analyses in TBM tunnel excavation: CEL and auto-remeshing approach", *Tunn. Undergr. Sp. Tech*., **116**, 104081. https://doi.org/10.1016/j.tust.2021.104081.

Kim, D. (2024), "Structural stability evaluation of TBM tunnels using numerical analysis approach", *Geomech. Eng*., **38**(6), 583-591. https://doi.org/10.12989/gae.2024.38.6.583.

Kim, D. and Jeong, S. (2021), "Estimation of the excavation damage zone in TBM tunnel using large deformation FE analysis", *Geomech. Eng*., **24**(4), 323-335. https://doi.org/10.12989/gae.2021.24.4.323.

Kim, D., Jeong, S. and Park, J. (2020), "Analysis on shaft resistance of the steel pipe prebored and precast piles based on field load-transfer curves and finite element method", *Soils Found*., **60**, 478-495. https://doi.org/10.1016/j.sandf.2020.03.011.

Kim, J., Ko, J. and Kim, D. (2023), "Analysis on inclined or rounded tip piles using 3D printing technology and FE analysis", *Geomech. Eng*., **33**(1), 91-99. https://doi.org/10.12989/gae.2023.33.1.091.

Korea Land and Housing Corporation. (2016), "Field design manual", Jinju.

Korea Meteorological Administration (2023), "2022 Abnormal climate report", Seoul.

Korea Presidential Water Commission. (2024), *Proceeding of the 1st Annual Seminar*, Seoul, February.

Kumara, J., Kurashina, T. and Kikuchi, Y. (2016), "Effects of pile geometry on bearing capacity of open-ended piles driven into sands", *Geomech. Eng*., **11**(3), 385-400. https://doi.org/10.12989/gae.2016.11.4.385.

Lee, C., Jeon, Y., Kim, S. and Park, I. (2016), "The influence of tunneling on the behavior of pre-existing piled foundations in weathered soil", *Geomech. Eng*., **11**(4), 553-570. https://doi.org/10.12989/gae.2016.11.4.553.

O'Neill, M., Townsend, F., Hassan, K., Buller, A. and Chan, P. (1996), "Load transfer for drilled shafts in intermediate geomaterials", Federal Highways Administration.

Orazalin, Z. (2017), "Analysis of large deformation offshore geotechnical problems in soft clay", Ph.D thesis, Massachusetts Institute of Technology, Cambridge MA, USA.

Orazalin, Z. and Whittle, A. (2018), "Realistic numerical simulations of cone penetration with advanced soil models", Cone Penetration Testing 2018, Delft, June.

Park, J. (2004), "Strength and friction behavior of cement paste poured in the bored pile", *J. Korean Geoenviron. Soc*., 5(3), pp. 31-39.

Reese, L. and O'Neill, M. (1988), "Drilled shafts: Construction procedures and design methods. Publication No. FHWA-HI-88-042", Federal Highway Administration, Washington, D.C.

Tian, Y., Cassidy, M.J., Randolph, M.F., Wang, D. and Gaudin, C. (2014), "A simple implementation of RITSS and its application in large deformation analysis", *Comput. Geotech*., **56**, 160-167. https://doi.org/10.1016/j.compgeo.2013.12.001.

Van Rossum, G. and Drake, F. (2006), Python reference manual.

Wang, D., Bienen, B., Nazem, M., Tian, Y., Zheng, J., Pucker, T. and Randolph, M. (2015), "Large deformation finite element analyses in geotechnical engineering", *Comput. Geotech*., **65**, 104-114. https://doi.org/10.1016/j.compgeo.2014.12.005.